International Journal of Nanomaterials and Chemistry

http://dx.doi.org/10.18576/ijnc/020102

# Synthesis and Study of Superparamagnetic ($Fe_3O_4$/ (Chitosan/alginate)-co-acrylic acid) Nanocomposite for Different Applications

Faten Ismail Abou El Fadl*

Egyptian Atomic Energy Authourity, Egypt

Received: 19 Nov. 2015, Revised: 9 Dec. 2015, Accepted: 14 Dec. 2015.
Published online: 1 Jan. 2016.

**Abstract:** In this article we report about the synthesis of superparamagnetic bare $Fe_3O_4$ nanostructures, (ALG/Chit/$Fe_3O_4$), and (ALG/Chit-co-AAc/$Fe_3O_4$) nanocomposites. The structural morphology and magnetic behavior of $Fe_3O_4$ nanostructures, (ALG/Chit/$Fe_3O_4$) and (ALG/Chit-co-AAc/$Fe_3O_4$) nanocomposites beads have been investigated by X-ray diffractometer (XRD), transmission electron microscopy (TEM), and scanning electron microscopy (SEM). The particle size was calculated by TEM measurements and it turns out to be 12.62, 6.9 and 5.5 nm for bare $Fe_3O_4$ nanoparticle, (ALG/Chit/$Fe_3O_4$) and (ALG/Chit-co-AAc/$Fe_3O_4$) nanocomposites beads, respectively. The synthesized $Fe_3O_4$ nanoparticle, (ALG/Chit/$Fe_3O_4$) and (ALG/Chit-co-AAc/$Fe_3O_4$) nanocomposites beads were found to be super parmagnetic in nature at room temperature.

**Keywords:** Alginate; Chitosan; Magnetite; TEM; XRD; Nano composite beads With best regards

## 1 Introduction

Magnetic nanoparticles (MNPs) investigations have attracted considerable attention to the scientists due to its application in various fields such as physics, medicine, biology and materials science. Particularly, superparamagnetic materials play an important role in biomedical applications including magnetic resonance imaging for clinical diagnosis, magnetic drug targeting, hyperthermia anti-cancer strategy [1-3] and enzyme immobilization [4,5]. Magnetite ($Fe_3O_4$) and maghemite (-$Fe_2O_3$) are the most commonly used magnetic carriers for a variety of biomedical applications [6].

Among the various types of magnetic materials, the magnetic–polymer composites represent a class of functional materials where magnetic NPs are embedded in polymer matrixes. Recently, a considerable number of studies have been done on magnetic–polymer nanocomposites such as; PVP-coated $Fe_3O_4$ [6], $Fe_3O_4$–chitosan and -$Fe_2O_3$ NPs [7, 4, 5], tyrosinase biosensor based on $Fe_3O_4$ NPs–chitosan nanocomposite [8], barium alginate caged $Fe_3O_4$/C18 magnetic NPs [9], polyaniline-coated nano-$Fe_3O_4$/carbon nanotube composite as the protein digestion [10], $Fe_3O_4$/PPy/P(MAA-co-AAm) trilayered composite [11], $Fe_3O_4$-PVA nanocomposites [12], polyaniline/nano-$Fe_3O_4$/composites [13], polymer–$Fe_3O_4$ nanocomposites [14], PEI modified $Fe_3O_4$/Au NPs [15], alginic acid–$Fe_3O_4$/nanocomposite [16].

Another form of polymer matrix is the smart polymer beads which attracted great interest in last decades. Smart polymer beads are designed to respond to the external stimuli [17, 18], e.g. temperature, pH, solvent composition, magnetic field etc. Among these stimuli, magnetic field has the additional advantages of instant action and contactless control. The sensitivity to magnetic field is provided by magnetic nano- or microparticles incorporated into the beads. Synthesis and properties of magnetic polymer beads constitute a new topic of research rapidly developing last 10 years. The magneto responsive polymeric beads benefit from the combination of features inherent to both their components: magnetic particles and polymer. The particles impart the magnetic properties to the beads. These properties allow for the rapid and easy separation of beads by the application of an external magnetic field.

As to the polymer component, it stabilizes the magnetic particles and offers swelling ability and elasticity to the beads. Also, polymer endows the particles with functional groups necessary for the desired applications. For example, functionalization of the surface of beads by specific ligands makes their usage possible in immunoassay methodologies [19], in the isolation of nucleic acid sequences [20], cells [21] and microorganisms [22] and also treatment of waste water. This work aimed at preparing polymer beads of chitosan and alginate by ionic crosslinking using divalent cations as $Ca^{+2}$ and grafting the ionically prepared (Chit/ALG) beads with acrylic acid by the effect of radiation to increase the polymer functionality.

* Corresponding author E-mail: fatenelramly555@yahoo.com

The magnetic (Chit/ALG) and the magnetic (Chit/ALG)-co-acrylic acid beads were obtained by embedding magnetic particles mainly ferrite in the form of $Fe_3O_4$ oxides where metal oxides are often preferred over pure metals (Fe, Co, and Ni) [23] because they are more stable to oxidation.

## 2 Experimental

### *2.1 Materials*

$FeCl_2$ and $FeCl_3 \cdot 6H_2O$ were used for the preparation of $Fe_3O_4$ NPs and its composites with chitosan/alginate beads, purchased from cornell lab for chemicals, Egypt, Chitosan powder with average molecular weight of 250 kDa, was purchased from Aldrish Co. The low viscosity alginic acid sodium salt was from Sigma, USA, acrylic acid (AAc) was purchased from Fluka. All reagents and salts were used without further purification. Doubly distilled water was used for solutions preparation.

### *2.2 Preparations and Characterizations*

### *2.2.1 Preparation of grafted alginate/chitosan beads*

Sodium alginate (Na–Alg) and chitosan in ultrapure water were prepared by weighting the respective solids to give (3 % wt/v) for each. Different compositions were prepared (50/50, 60/40, 80/20, and 90/10, Alg/Chit) under magnetic stirring until became homogeneous. Using a 10 ml syringe the Na–Alg and ALG/Chit different compositions were transferred drop wise from a distance of 10 cm into a solution of $CaCl_2.2H_2O$ (3 % wt/v) which was under magnetic stirring. Hydrogel beads were formed instantly and they were left in contact with the solution for 30 min in order to complete the gelation. Finally they were rinsed gently with ultrapure water and dried at 37 $^oC$. Then crosslinked alginate/chitosan beads are immersed in acrylic acid (AAc) of concentration 40 % at room temperature for 24 h, and after that, exposed to irradiation using Co 60 gamma source. After irradiation, the grafted chitosan/alginate beads (alginate/chitosan-co32-AAc) were washed in boiling water to remove un-reacted monomer and homopolymer then air dried to constant weight. The grafting yield was calculated as follows

$$G\% = (W_g - W_0)/W_0 \quad (1)$$

Where, $W_g$ is the weight of beads after grafting, $W_o$ is the weight of beads before grafting.

### *2.2.2 Preparation of $Fe_3O_4$ nanoparticles*

Co-precipitation technique is used to synthesize $Fe_3O_4$ as previously reported with some modifications [9]. Briefly, 5.8 g of $FeCl_3 \cdot 6H_2O$ dissolved in 200 mL of distilled water afterwards $FeSO_4 \cdot 7H_2O$ of 2.1 g were also dissolved in the mixture and heated to 60 °C, then $NH_4OH$ (28%) was added rapidly, and pH of the solution was maintained at 10.0. The suddenly obtained precipitate was filtered and washed several times to remove the impurities of chloride ions. The washed precipitate was drying in vacuum to get the final products.

### *2.2.3 Preparation of magnetic nanocomposite beads*

The magnetic nanocomposites beads were prepared by placing the previously prepared (ALG/Chit) and (ALG/Chit)-co-AAc beads individually in 50 ml of double distilled water and allowed them to swell completely over a period of 24 h. Each individual bead sample was then transferred separately to another beaker containing 200 ml of water consisting of 2.1g of Fe $Cl_2$. $4H_2O$ and 5.8 g of Fe $Cl_3$. $6H_2O$ and allowed it for 24h to entrap the iron salts throughout the hydrogel networks. Then the beads loaded with iron (II) and iron (III) ions were removed from the iron salt solutions, washed with double distilled water and placed in a beaker consisting of 50 ml of 0.5 M sodium hydroxide solution and left tell dark brown beads are obtained. The resultant brown or black color magnetic nanocomposite beads Fig.1 were removed, washed with double distilled water, and allowed to dry in an oven at 60°C. The properties of the final product depend on some parameters such as the ratio between $Fe^{2+}$ and $Fe^{3+}$, pH and ionic strength of the medium.

### *2.3 Morphological studies*

### *2.3.1 Scanning electron microscopy (SEM)*

The surface morphology of different alginate/chitosan and (alginate/chitosan)-g-AAc samples were taken with a JSM-5400 instrument by JEOL-Japan. A sputter coater was used to pre-coat conductive gold onto the surface before observing the microstructure at 10 kV.

### *2.3.2 Transmission electron microscopy (TEM)*

Transmission electron microscopy (TEM) was performed with a JEOL 100CX JEM operating at 80 kV. It is used to determine the size of iron nanoparticles inside the polymeric beads. To image the magnetic nanoparticles on the TEM, finely ground beads samples were dispersed in 1 ml of ethanol and then they sonicated to get a solution of magnetic nanoparticles. Approximately 10–20 μl of this solution was dropped onto a 3 mm copper grid, which was then dried at room temperature. Finally, the copper grid was inserted into the transmission electron microscope.

### *2.3.3 X-Ray Diffraction*

X-ray diffraction was used to identify the magnetic nanoparticles into the polymeric matrix. These

measurements were carried out on a Shimadzu (Kyoto, Japan) X-ray diffractometer (XRD-6000 model) equipped with an X-ray tube (Cu target), and using a voltage of 40 kV and a current of 30 mA.

## 3 Results and Discussion

The formation of the ALG/Chit beads is mainly based on the ability of alginate for gelation with divalent cations like $Ca^{2+}$ which is ionically crosslink carboxylate groups in the G-block of alginate. The grafting of acrylic acid to the ALG/Chit beads was achieved by the effect of gamma radiation to increase the functionality of the polymer beads. The magnetic nanoparticles ($Fe_3O_4$) were synthesized as mentioned above. The following equations show the steps of formation of magnetite particles into the polymeric beads:

$$Fe^{2+} + Fe^{3+} \rightarrow Fe(OH)_2 + Fe_2O_3 \cdot H_2O \rightarrow Fe_3O_4 + H_2O \quad (1)$$

$$Fe(OH)_2 = Fe\,OH^+ + OH^- (+HFeO^{2-}) \quad (2)$$

$$Fe\,OH^+ + O_2 \rightarrow [Fe_2(OH)_3]^{3+} \quad (3)$$

$$[Fe_2(OH)_3]^{3+} + Fe\,OH^+ \rightarrow Fe_3O_4 \quad (4)$$

In this paper, a facile chemical method was developed to prepare (ALG/Chit)/$Fe_3O_4$) and (ALG/Chit-co-AAc)/$Fe_3O_4$ with narrow size distributions using modified co-precipitation method. Figure 1 illustrates the digital images of (ALG/Chit), (ALG/Chit-co-AAc) and their magnetic beads.

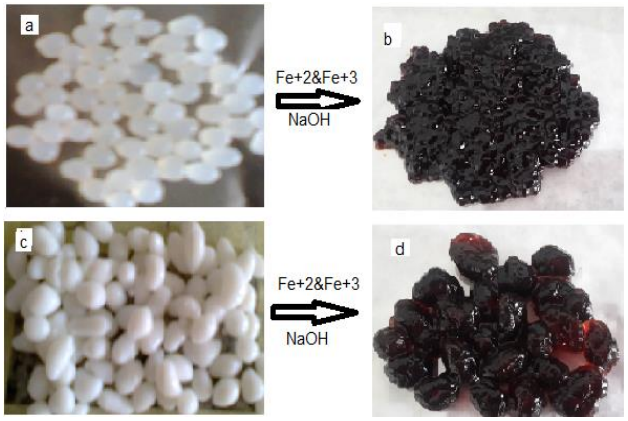


**Figure 1:** digital photos of a) (ALG/Chit) beads and d) (ALG/Chit)-co-AAc represent the change in color after imbedding $Fe_3O_4$ NPs

### *3.1 Magnetic properties*

It should be emphasized that the size of iron oxide particles plays an essential role in their behavior in magnetic field [24]. Small particles possess single domain structure. Single domains include groups of spins all pointing in the same direction and acting cooperatively. By contrast, larger particles possess multi domain structure consisting of many single domains separated by domain walls, which produce magnetic flux closures rendering the bulk material macroscopically non-magnetic [25]. Figure 2 below illustrates the magnetization curves for pare $Fe_3O_4$ and (ALG/Chit)-co-AAc/$Fe_3O_4$ nanocomposite beads. It is obvious from this figure that (ALG/Chit)-co-AAc/$Fe_3O_4$ nanocomposite beads can be considered super paramagnetic material also, it is clearly noticed that the magnetic saturation of (ALG/Chit)-co-AAc/$Fe_3O_4$ nanocomposite beads is lower than that of pare $Fe_3O_4$ NPs.

This may attributed to the coating effect of alginate and chitosan on the $Fe_3O_4$ NPs trapped in the gel matrix. The ferromagnetic behavior of synthesized (ALG/Chit)-co-AAc/$Fe_3O_4$ nanocomposite beads means that they have strong magnetic responsively and can be separated easily from the solution with the help of an external magnetic force which make it applicable in many fields.

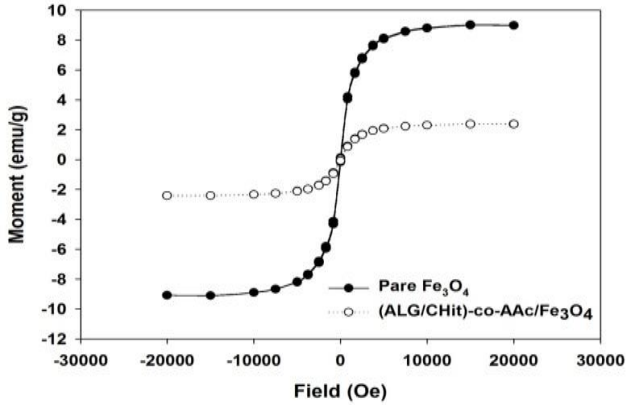


**Figure 2:** Magnetic hysteresis loops of pare $Fe_3O_4$ NPs and (ALG/Chit)-co-AAc/$Fe_3O_4$

### *3.2 Scanning Electron Microscopy (SEM)*

SEM is used to study and recognize the morphological change after grafting of AAc into ALG/Chit beads by using gamma radiation and also the morphological change due to imbedding of $Fe_3O_4$ NPs into both (ALG/Chit) and (ALG/Chit)-co-AAc prepared beads. Figure 3 below illustrates the SEM micrographs of a) (ALG/Chit), b) (ALG/Chit)-co-AAc, c) (ALG/Chit)/$Fe_3O_4$ and d) (ALG/Chit)-co-AAc/$Fe_3O_4$. It is obvious from the figure the change in the fracture surface of (ALG/Chit) beads (Fig 2a) after grafting with acrylic acid where the surface became more rough and not homogeneous (Fig 2b).

The surface of the (ALG/Chit) after embedding $Fe_3O_4$ NPs completely changed to a surface full of very small pores indicating the presence and formation of $Fe_3O_4$ NPs that supposed to be trapped in this pores (Fig 2c). The surface morphology of the (ALG/Chit-co-AAc) totally changed after embedding of $Fe_3O_4$ NPs where the surface became full of very tiny holes and cavities due to adsorption and formation of $Fe_3O_4$ NPs (Fig 2d).

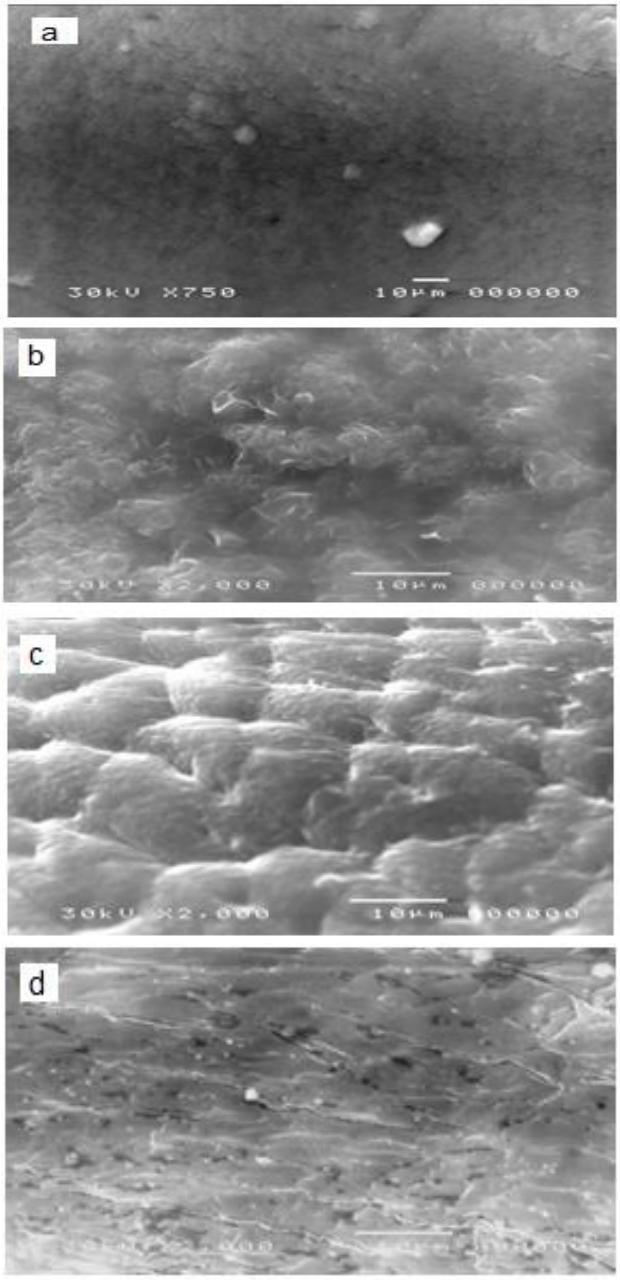


**Figure 3:** SEM micrographs of a) (ALG/Chit), b) (ALG/Chit-co-AAc), c) (ALG/Chit)/$Fe_3O_4$, and d) (ALG/Chit)-co-AAc/ $Fe_3O_4$ magnetic nanocomposite beads

### *3.3 Transmission Electron Microscopy (TEM)*

Figure 3 shows the TEM images of $Fe_3O_4$ nanoparticles, (ALG/Chit)/$Fe_3O_4$, and (ALG/Chit)-co-AAc/ $Fe_3O_4$ magnetic nanocomposite beads. It is obvious from these images that the size and shape of $Fe_3O_4$ is affected by changing the polymer environment. The TEM image of bare $Fe_3O_4$ NPs shows unfixed and not regular shape with size of (12.62 nm) as clearly obvious in figure 3a. Figure 3b represents the TEM image of (ALG/Chit)/$Fe_3O_4$ where it is clear that the $Fe_3O_4$ particles distributed uniformly throughout the hole surface and also, the shape of the particles became more regular, while on the other hand, the distribution of $Fe_3O_4$ NPs throughout the (ALG/Chit)-co-AAc/ $Fe_3O_4$ magnetic nanocomposite beads surface is not uniform completely and there is some agglomerations depicted on the surface due to grafting of acrylic acid (Fig 3c). From comparing the shape and the size depicted from the TEM images it is important to notice that embedding the $Fe_3O_4$ NPs inside the (ALG/Chit) and (ALG/Chit)-co-AAc beads resulted in a more spherical and small sized particles (6.9 and 5.5 nm respectively) than the pare $Fe_3O_4$ NPs (12.62 nm).

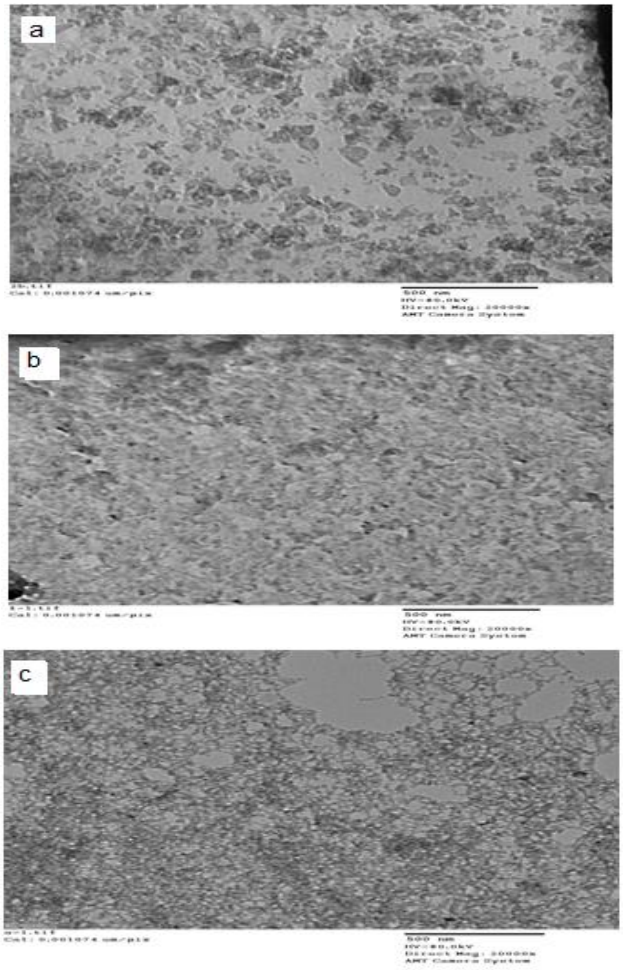


**Figure 4:** TEM images of a) pare $Fe_3O_4$, b) ALG/Chit)/$Fe_3O_4$, and c) (ALG/Chit)-co-AAc/ $Fe_3O_4$ nanocomposite beads.

**X-Ray diffraction of magnetic (CS/ALG) and magnetic (CS/ALG-co-AAc)**

In Fig 5 the XRD patterns of (ALG/Chit), (ALG/Chit/$Fe_3O_4$), and (ALG/Chit)-co-AAc/ $Fe_3O_4$ reveals similar characteristic peaks with pure $Fe_3O_4$ nanoparticles, which confirm the formation of $Fe_3O_4$ particles. Comparing to single phase $Fe_3O_4$ NPs, Six characteristic peaks for

magnetite (2θ = 30.1, 35.5, 43.1, 53.4, 57.0, and 62.6°) [26] in the XRD patterns. The (ALG/Chit/$Fe_3O_4$), and (ALG/Chit)-co-AAc/ $Fe_3O_4$ nanocomposites beads show an amorphous feature by the presence of peak at (2theta = 20◦) along with the low intensity of the other peaks. This is attributed to the introduction of amorphous shell of alginate and chitosan [27].

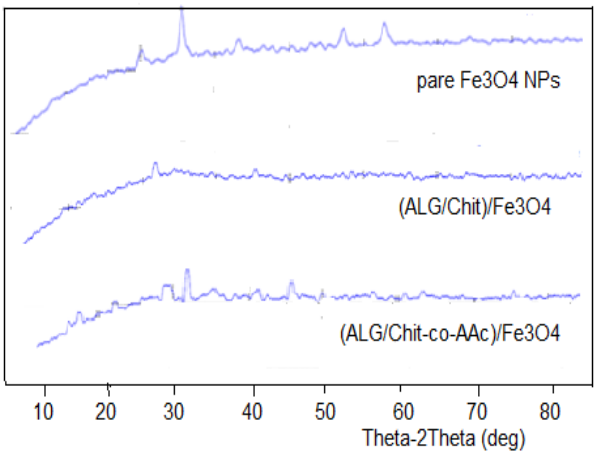


**Figure 5:** XRD patterns of pare $Fe_3O_4$, (ALG/Chit)/$Fe_3O_4$, and (ALG/Chit-co-AAc)/$Fe_3O_4$

## Conclusion

Super paramagnetic bare $Fe_3O_4$ NPs and (ALG/Chit/$Fe_3O_4$), and (ALG/Chit)-co-AAc/ $Fe_3O_4$ nanocomposites beads were synthesized by coprecipitation and in situ coprecipitation respectively. The TEM micrographs revealed that the $Fe_3O_4$ NPs have unfixed shape and homogeneously dispersed in the (ALG/Chit/$Fe_3O_4$) beads but on the other hand, the $Fe_3O_4$ distribution within (ALG/Chit)-co-AAc/ $Fe_3O_4$ nanocomposites beads was restricted by polymer matrix and the possible interaction of NPs with the polymer chains. The magnetization measurements of (ALG/Chit/$Fe_3O_4$), (ALG/Chit)-co-AAc/ $Fe_3O_4$ and the strong attraction of the prepared $Fe_3O_4$ NPs to a magnetic bar show that the synthesized products are super paramagnetic in nature at room temperature. The synthesized super paramagnetic NPs and its composite with biocompatible chitosan/alginate matrix can be used in various types of environmental and biomedical applications.

## References

[1] Gupta, A. K., & Gupta, M. Synthesis and surface engineering of iron oxide nanoparticles for biomedical applications. Biomaterials, 26(18), (2005); 3995–4021.

[2] Kim, G. C., Li, Y. Y., Chu, Y. F., Cheng, S. X., Zhuo, R. X., & Zhang, X. Z. Nanosized temperature-responsive $Fe_3O_4$-UA-g-P(UA-co-NIPAAm) magnetomicelles for controlled drug release. European Polymer Journal, 44(9), (2008); 2761–2767.

[3] Qu, J., Liu, G., Wang, Y., & Hong, R. Preparation of $Fe_3O_4$–chitosan nanoparticles used for hyperthermia. Advanced Powder Technology, 21(4), (2010); 461–467.

[4] Singh, J., Kalita, P., Singh, M. K., & Malhotra, B. D. Nanostructured nickel oxide-chitosan film for application to cholesterol sensor. Applied Physics Letters, (98), (2011); 123702–123704.

[5] Singh, J., Srivastava, M., Dutta, J., & Dutta, P. K. Preparation and properties of hybrid monodispersed magnetic α-$Fe_2O_3$ based chitosan nanocomposite film for industrial and biomedical applications. International Journal of Biological Macromolecules, 48(1), (2011); 170–176.

[6] Liu, H. L., Ko, S. P., Wu, J. H., Jung, M. H., Min, J. H., Lee, J. H., et al. One-pot polyol synthesis of monosize PVP-coated sub-5 nm $Fe_3O_4$ nanoparticles for biomedical applications. Journal of Magnetism and Magnetic Materials, 310(2), (2007); 815–817.

[7] Li, G., Jiang, Y., Huang, K., Ding, P., & Chen, J. Preparation and properties of magnetic $Fe_3O_4$–chitosan nanoparticles. Journal of Alloys and Compounds, 466(1–2), (2008); 451–456.

[8] Wang, S., Bao, H., Yang, P., & Chen, G. Immobilization of trypsin in polyanilinecoated nano-$Fe_3O_4$/carbon nanotube composite for protein digestion. Analytica Chimica Acta, 612(2), (2008); 182–189.

[9] Zhang, C., Shi, J., Yang, X., De, L., & Wang, X. Effects of calcination temperature and solution pH value on the structural and magnetic properties of $Ba_2Co_2Fe_{12}O_{22}$ ferrite via EDTA-complexing process. Materials Chemistry and Physics, 123(2-3), (2010); 551–556.

[10] Wang, S., Tan, Y., Zhao, D., & Liu, G. Amperometric tyrosinase biosensor based on $Fe_3O_4$ nanoparticles–chitosan nanocomposite. Biosensors and Bioelectronics, 23(12), (2008); 1781–1787.

[11] Luo, Y. L., Fan, L. H., Xu, F., Chen, Y. S., Zhang, C. H., & Wei, Q. B. Synthesis and characterization of $Fe_3O_4$/PPy/P (MAA-co-AAm) trilayered composite microspheres with electric, magnetic and pH response characteristics. Materials Chemistry and Physics, 120(2-3), (2010); 590–597.

[12] Liu, T. Y., Hu, S. H., Liu, K. H., Liu, D. M., & Chen, S. Y. Study on controlled drug permeation of magnetic-sensitive ferrogels: Effect of $Fe_3O_4$ and PVA. Journal of Controlled Release, 126(3), (2008); 228–236.

[13] Xiao, Q., Tan, X., Ji, L., & Xue, J. Preparation and characterization of polyaniline/nano-Fe3O4 composites via a novel Pickering emulsion route. Synthetic Metals, 157(18–20), (2007); 784–791.

[14] Yang, T., Brown, R. N. C., Kempel, L. C., & Kofinas, P. Magneto-dielectric properties of polymer–$Fe_3O_4$ nanocomposites. Journal of Magnetism and Magnetic Materials, 320(21), (2008); 2714–2720.

[15] Sun, H., Zhu, X., Zhang, L., Zhang, Y., & Wang, D. Capture and release of genomic DNA by PEI modified $Fe_3O_4$/Au nanoparticles. Materials Science and Engineering C, 30(2), (2010); 311–315.

[16] Unal, B., Toprak, M. S., Durmus, Z., Sozeri, H., & Baykal, A. Synthesis, structural and conductivity characterization of

alginic acid–$Fe_3O_4$ nanocomposite. Journal of Nanoparticle Research, 12(8), (2010); 3039–3048.

[17] Philippova OE. Responsive polymer gels. Polymer Science C 42(2), (2000); 208–28.

[18] Kramarenko EYu, Philippova OE, Khokhlov AR. Polyelectrolyte networks as highly sensitive polymers. Polym Sci C 48(1), (2006); 1–20.

[19] Guesdon JL, Avrameas S. Magnetic solid-phase enzyme immunoassay for the quantitation of antigens and antibodies: application to human immunoglobulin E. Methods Enzymol (73) (1981); 471–82.

[20] Albretsen C, Kalland K-H, Haukanes B-I, Havarstein LS, Kleppe K. Applications of magnetic beads with covalently attached oligonucleotides in hybridization: isolation and detection of specific measles virus mRNA from a crude cell lysate. Anal Biochem 189 (1), (1990); 40–50.

[21] Vardtal F, Gaudernack G, Funderud S, Bratlie A, Lea T, Ugelstad J, et al. HLA class I and II typing using cells positively selected from blood by immunomagnetic isolation – a fast and reliable technique. Tissue Antigens 28(5), (1986); 301–12.

[22] Safarik I, Safarikova M, Forsythe SJ. The application of magnetic separations in applied microbiology. J Appl Bacteriol (78), (1995); 575–85.

[23] Schmidt AM. Thermo responsive magnetic colloids. Colloid Polym Sci (285), (2007); 953–66.

[24] Chatterjee J, Haik Y, Chen CJ. Size dependent magnetic properties of iron oxide nanoparticles. J Magn Magn Mater 257(1), (2003); 113–8.

[25] Papaefthymiou GC. Nanoparticle magnetism. Nano Today 4(5), (2009); 438–47.

[26] Ravindra Kumar Gautam, Pavan Kumar Gautam, Sushmita Banerjee, Shivani Soni, Sanjeev K. Singh, Mahesh Chandra Chattopadhyaya, Removal of Ni (II) by magnetic nanoparticles. Journal of Molecular Liquids (204), (2015); 60–69.

[27] Fang, F. F., Kim, J. H., & Choi, H. J. Synthesis of core–shell structured PS/$Fe_3O_4$ microbeads and their magnetorheology. Polymer, 50(10), (2009); 2290–2293.